Spontaneous Fractal Aggregation of Gold Nanoparticles and Controlled Generation of Aggregate-Based Fractal Networks at Air/Water Interface

Wenlong Cheng,[†,§] Shaojun Dong,[*,†] and Erkang Wang[*,†]

State Key Laboratory of Electroanalytical Chemistry, Changchun Institute of Applied Chemistry, Chinese Academy of Sciences, Changchun, Jilin, 130022, P.R. China, and Graduate School of the Chinese Academy of Sciences, Beijing, 100039, P.R. China

Received: May 1, 2005; In Final Form: July 12, 2005

The spontaneous fractal aggregation of as-prepared cetytrimethylammonium bromide (CTAB)-capped gold nanoparticles was found to happen at the air/water interface after spreading their chloroform solution on water surfaces. Aided by Langmuir−Blodgett techniques, these fractal aggregates can be interconnected with each other to form aggregate-based fractal networks.

Introduction

Many macroscopically visible objects in nature, such as trees, coastlines, patterns of stars, etc., share a hidden symmetry. Mandelbrot[1] was the first to recognize this kind of complex symmetry and called it fractal geometry. A fractal object is an object that is self-similar, i.e., the structure of the object is invariant under a transformation which replaces a small part by a bigger part. Microscopically, fractal morphology was also found to be very common for particle aggregates including soot, silica, latex, clay, etc.[2] Among them, fabrication of fractal structures from metallic nanoparticles was especially important due to their novel physiochemical properties[3] and applications in surface-enhanced Raman scattering.[4] In solution, fractal nanoparticle aggregates were fabricated usually by the addition of some promotors such as phthalazine,[5] pyridine,[6] gelatin,[7] DNA,[8] etc. The promoters usually displace native charged ligands and adsorb strongly on nanoparticle surfaces, which reduces the repulsive forces between the charged nanoparticles. As a result, destabilized nanoparticles would stick to each other and form fractal structures when they collide. The fractal metallic structures can also be fabricated directly on solid supports by in situ reduction of gold salts.[9] More interestingly, it was found that the fractal gold nanoparticle aggregates can also be fabricated at the air/water interface by thermal induction[10] or the LB technique.[11]

Herein, we found that as-synthesized CTAB-capped gold nanoparticles can aggregate rapidly into fractals after spreading their chloroform solution on water surfaces. These fractal aggregates are hydrophobic showing a large moving freedom on water surfaces. They can be pushed together by the LB baffles in a similar way to the nanoscopic "logs-on-a-river".[12] At intermediate surface pressures, these fractal aggregates coalesced into large aggregate-based networks, which are also fractal in structure. TEM studies indicated that the original fractal aggregates are robust, and their structures were nearly kept at intermediate surface pressures. At surface pressures further elevated to near collapse pressure, a plastic-like thin film formed at the water surfaces and fractal structures were destroyed.

Experimental Section

Chemicals. $HAuCl_4 \cdot 3H_2O$ (Shanghai Chemical Plant), chloroform (Beijing Chemical Plant), sodium borohydride (ACROS), and cetyltrimethylammonium bromide (Beijing Chemical Plant) were used as received. All aqueous solutions were prepared by high-purity deionized water. Pure water for the subphase was first deionized and then distilled.

Synthesis of CTAB-Capped Gold Nanoparticles in Choroform. $HAuCl_4$ can be transferred into organic solvent by virtue of ion-pair extraction.[13] Previously, we have shown that CTAB can also carry gold salts from water into toluene.[14] Here, it was found that it is more efficient to transfer gold salts from water into chloroform, and a nearly complete transfer was achieved. Subsequent reduction by sodium borohydride generated more stable gold nanoparticles. Briefly, the preparative process is described as follows: CTAB-capped gold nanoparticles were prepared on a two-phase chloroform/water system. Then, 2 mL of a 1% aqueous solution of hydrogen tetrachloroaurate was mixed with 60 mL of saturated CTAB chloroform solution under vigorous stirring. The hydrogen tetrachloroaurate can be transferred nearly totally from water into chloroform, resulting in a deep orange solution. Then, the chloroform phase was separated, and freshly prepared aqueous sodium borohydride solution was added dropwisely into the stirred chloroform solution until the color of the organic phase changed from deep orange to ruby red. After further stirring for 30 min, the ruby red chloroform solution was extracted and washed with deionized water 3 times. The resulting ruby solutions were stored in the dark at 4 °C. The colloidal solutions were very stable and show no sign of a precipitate even after 1 year.

Langmuir−Shaefer Films on Mica and Carbon-Coated Copper Grid. A volume of 300 μL of the as-prepared CTAB-capped gold nanoparticles (~0.47 mg/mL) was spread carefully on the surface of pure water in the LB trough at 20 °C. The surface pressure was monitored using the Wilhelmy plate method. Compression of the film was done at a rate of 10 mm/min after the choroform was evaporated (10 min). The LB films were transferred onto freshly cleaved mica for AFM studies or

* Corresponding authors. E-mail: ekwang@ciac.jl.cn.
[†] Changchun Institute of Applied Chemistry, Chinese Academy of Sciences.
[§] Graduate School of the Chinese Academy of Sciences.

10.1021/jp052255a CCC: $30.25
Published on Web 09/24/2005

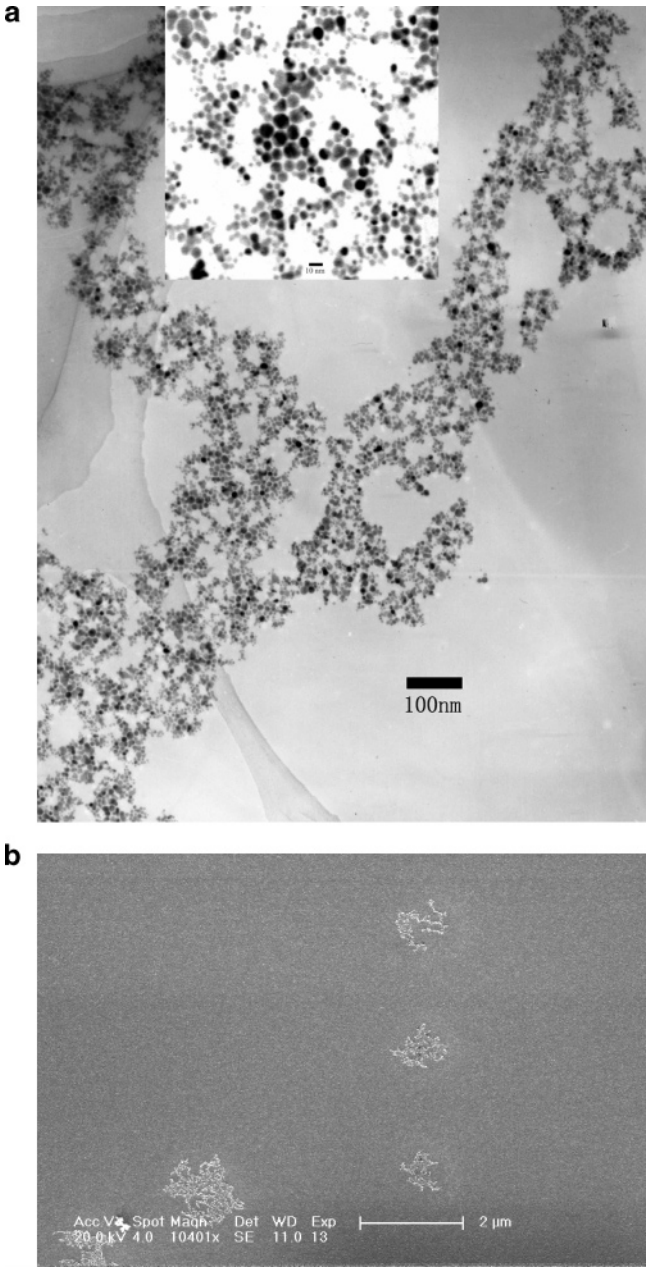

Figure 1. (A) TEM image of the spontaneously generated fractal aggregates supported on a carbon-coated copper grid. (B**)** FESEM image of the spontaneously generated fractal aggregates transferred on a mica surface.

clean glass slides for optical studies or carbon-coated copper grids for TEM studies by horizontal liftoff (i.e., the Langmuir−Scharffer technique[11]).

Instrumentation. The UV−vis absorbance spectra were acquired using a Cary 500 UV−vis NTR spectrometer (Varian, U.S.A.). LB films of the as-prepared gold nanoparticles were made using a KSV 5000 Langmuir trough. The electronic images were made on a JEOL 2010 transmission electron microscope operating at 200 kV. AFM images were taken by using a Nanoscope IIIa instrument operating in the tapping mode with standard silicon nitride tips. Typically, the surface was scanned at 2 Hz with 256 lines per image resolution and 1.0−2.0 V set point.

Result and Discussion

When a drop of the as-synthesized red-gold colloid in chloroform was spread on water surfaces, a blue-colored

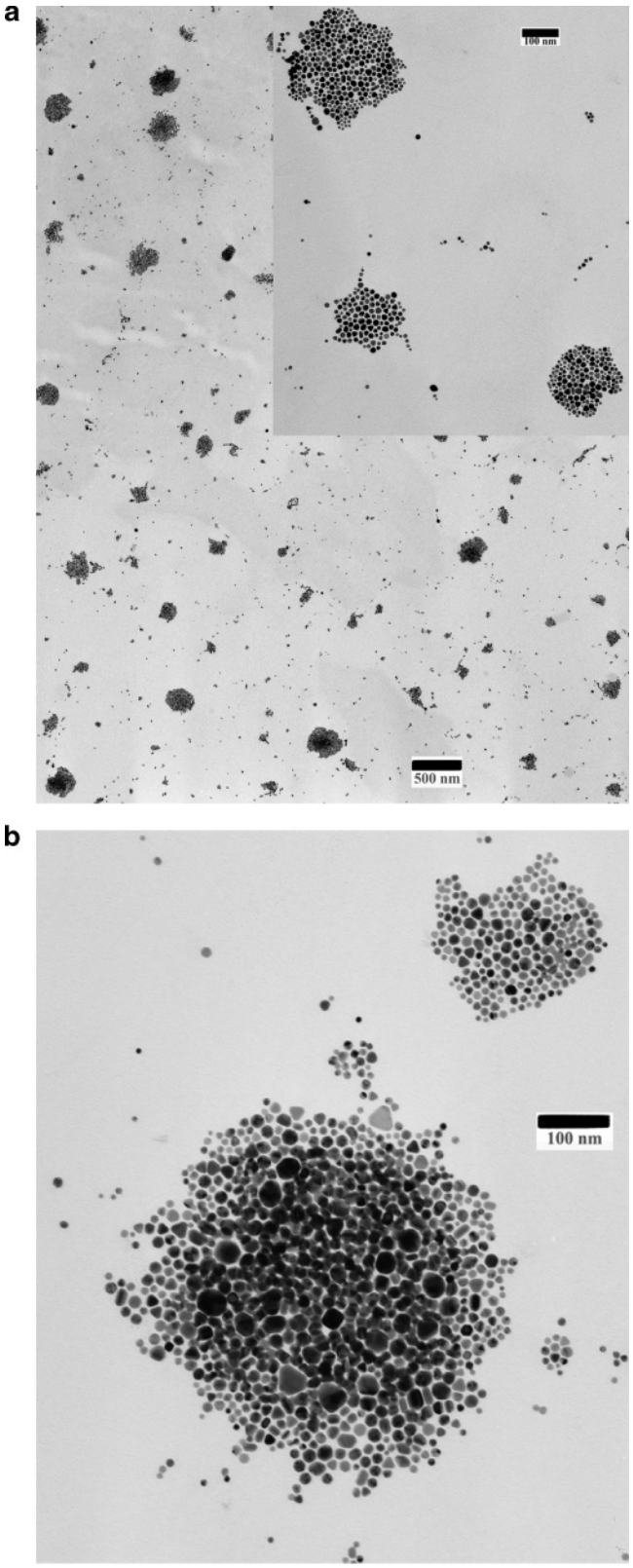

Figure 2. (A) TEM image of the as-synthesized CTAB-capped gold nanoparticles on a carbon-coated copper grid. Inset: enlarged view of three 2D aggregates. (B) TEM image of the as-synthesized CTAB-capped gold nanoparticles on a carbon-coated copper grid illustrating their fusion in some domains.

discontinuous film formed immediately after. The color changes indicate extensive nanoparticle aggregation.[15] In fact, the formation of aggregates can be explained very well by the recently developed integral equation theory of solvent-induced potential of mean force between two passivated nanoparticles.[16]

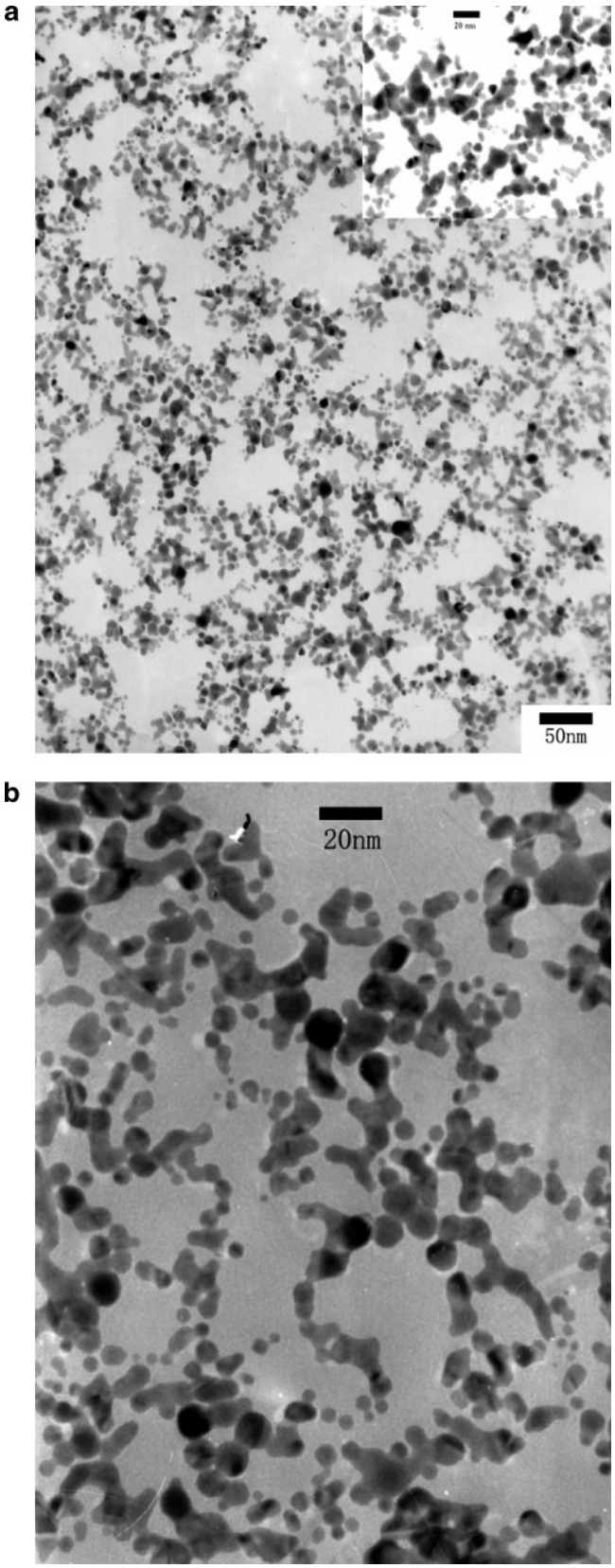

Figure 3. TEM images of the observed fusing quasi-1D nanostructures at surface pressures of 0 mN/m (a) and 13 mN/m (b).

The CTAB-capped gold nanoparticles are solvophilic with respect to choroform and solvophobic with respect to water and air. The drying of the choroform would force the nanoparticles into a solvophobic environment (air/water interface), therefore, enhancing the solvophobic attractive forces between nanoparticles. Because the contact between hydrophobic gold nanoparticles and water surfaces is incompatible, the nanoparticles are highly movable. Thus, aggregation happened rapidly by the strong solvophobic attractions.

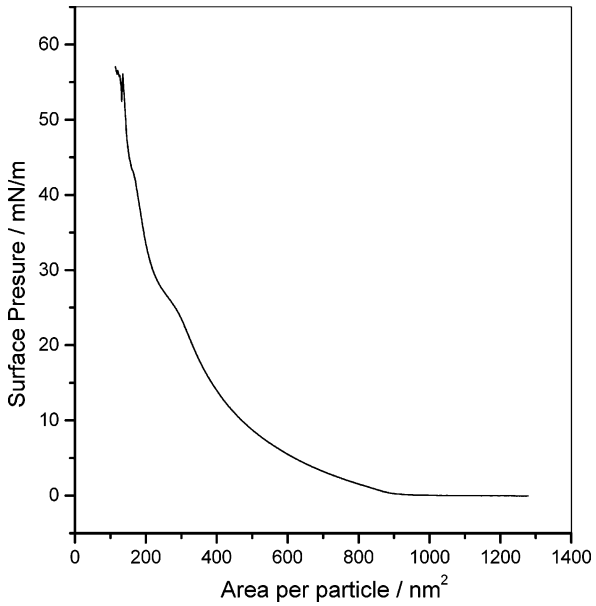

Figure 4. Typical compression isotherm of an LB film of CTAB-capped gold nanoparticles.

To gain insight into the aggregating structure, the film was transferred carefully onto a carbon-coated copper grid for TEM characterization or onto mica for FESEM characterization by horizontal liftoff. Figure 1A shows a typical TEM micrograph of an aggregate, which reveals a highly ramified, extended, and open structure. Obviously, the aggregate is fractal in structure, following possibly a diffusion-limited growth mechanism.[2−4] Figure 1B shows a typical FESEM micrograph of the transferred Langmuir−Schaefer films on mica. Several well-separated aggregates in the micrometer range were clearly observed. Any single aggregate can be identified as a fractal. As a control, we also characterized the gold nanoparticle films formed on a carbon-coated grid by directly dispersing chloroform solution on it. In our studies, fractals of gold nanoparticles were never observed. Figure 2A shows a representative TEM image of the thus-prepared nanoparticle films. Obviously, fractal-like structures are absent instead of some spherelike aggregates from the gold nanoparticles and some discrete nanoparticles. The high-resolution image of these aggregates (inset of Figure 2A) shows that most of the gold nanoparticles are well-separated from each other. The fusion of the gold nanoparticles (Figure 2B) was observed only in some big aggregates. The fusion was more pronounced in the center of the big aggregates in Figure 2B. This indicates that fusion might happen at the final stage of chloroform evaporation. The gold nanoparticles were destabilized due to a high local concentration. For the nanoparticles with a low concentration, nanoparticle fusion was scarcely observed, showing a relatively good stability. From the control experiments, in addition, it can be concluded obviously that the fractal aggregation of the gold nanoparticles happened at the air/water interface rather than on the carbon-coated copper grid.

With the use of the box-counting method,[17] the fractal dimension in Figure 1 was estimated as ∼1.87 (see the Supporting Information). Liu et al. have reported that the nanoparticle fractal dimension (*D*) is an indication of the large interparticle attraction energy.[17] *D* increases as the interparticle attraction energy is decreased. According to their result, it was thought that the interparticle attraction energy should be large.

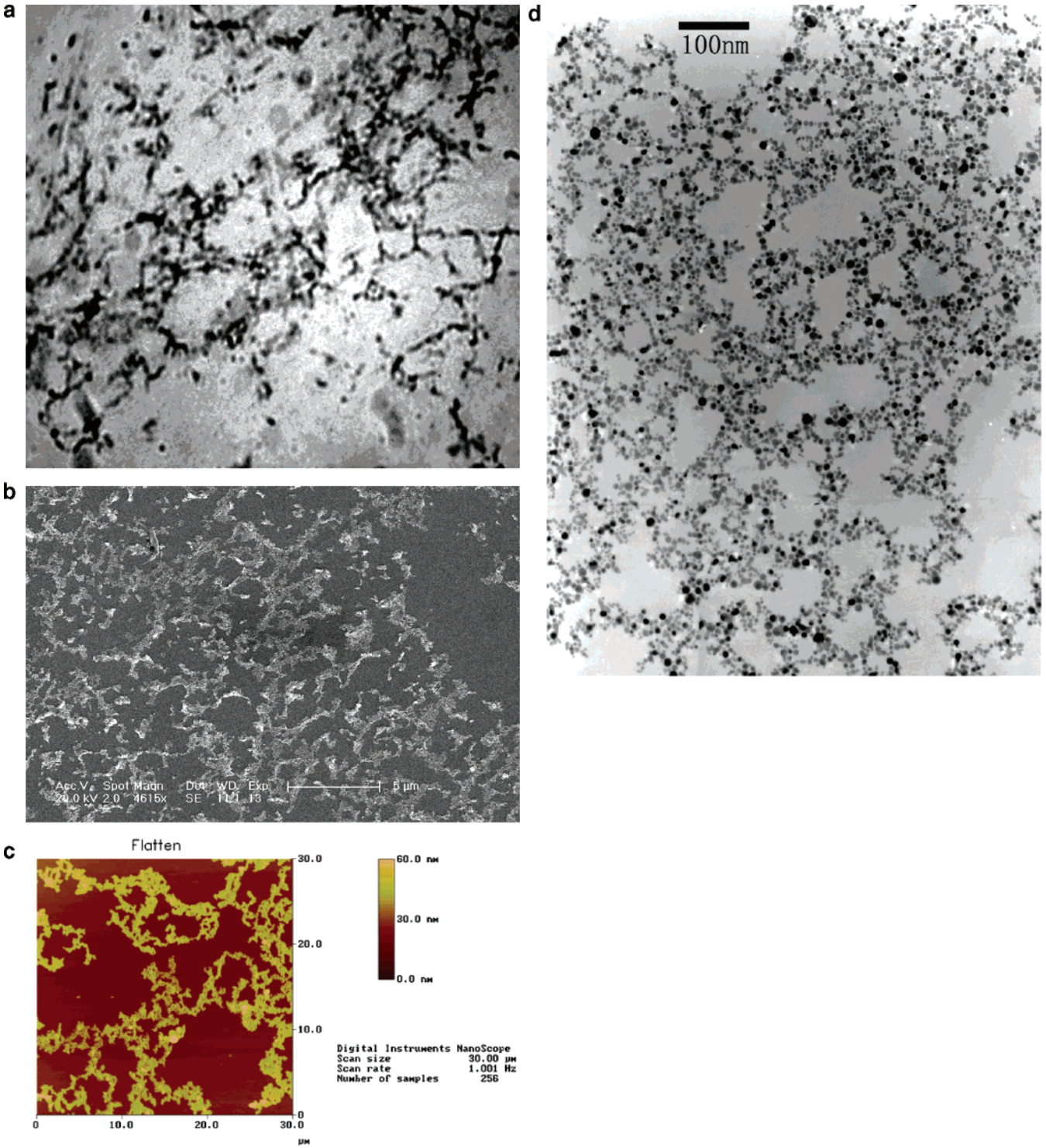

Figure 5. Morphological characterization of aggregate-based fractal networks formed at intermediated surface pressures (13−30 mN/m). The fractal structures are highly reproducibly as observed on the centimeter-to-micrometer scale by several tools: (a) optical microscope image; (b) FESEM image; (c) tapping mode AFM image; (d) SEM image.

The enlarged view of the fractal (Figure 1A) supports the strong sticking interactions between nanoparticles. Only a small amount of nanoparticles were kept separate. Most nanoparticles are nearly in direct contact, and even some nanoparticles have fused into quasi-1D nanowires or nanoflakes.

The efficient sticking upon contact might come from the limited stability of the CTAB-capped gold nanoparticles at the air/water interface. It is known that the capping interactions between CTAB molecules and gold nanoparticles are electrostatic. These interactions are weaker than those between alkylthiol[11] or alkylamine[18] and metal surfaces. In chloroform, the CTAB-capped gold nanoparticles are in an extremely stable dynamic state. This is not the case at the air/water interface. CTAB molecules can form monolayers by adsorbing on water surfaces or dive into water to form reverse micelles at the air/water interface. The chloroform evaporation forces hydrophobic nanoparticles to accumulate locally, and strong drying-mediated collision would result in dislocation of the capping CTAB molecules from the gold surfaces by adsorbing on water surfaces and diving into water. The removal of the capping CTAB molecules renders the gold nanoparticles partially unprotected; as a result, the gold nanoparticles have to fuse into larger

structures to lower the surface-to-volume ratio to decrease the surface energy.[11b,19] The dispersion attractions among gold nanoparticles act as driving factors for the fusing process; whereas, the nanoparticle surface-bound CTAB molecules counteract this fusing process because it has to overcome the electrostatic repulsion between positively charged CTAB amino groups and withdraw hydrophobic alkyl chains. When the driving and counteracting interactions are balanced, the nanoparticles stop fusing. Besides the efficient sticking interactions, incompatible contact between hydrophobic nanoparticles and the water interface might play also a role for the formation of fractals. This incompatible contact enables nanoparticles to diffuse at will on water surfaces. This might be another precondition of growth of nanoparticles into fractal aggregates.[2] It was thought that the sticking interactions between nanoparticles and the carbon-coated copper grid are strong enough to prevent them from walking randomly on carbon surfaces. As a result, the fractal aggregates of the gold nanoparticles were never observed directly on carbon surfaces.

It was also noted that fusion was more pronounced, as shown in Figure 3a, in some domains. This indicates that the aggregating/fusing process might be rapid and irreversible, which would result in a different local environment. The elevated surface pressures seem to favor the nanoparticle fusion; larger fused quasi-1D nanowires were observed as shown in Figure 3b. It was thought that the elevated surface pressures are favorable for the CTAB removal in a similar way as that discussed in ref 11b. A difference is that the nanoparticle fusion reported here is a spontaneous evaporation-induced process, not a result of exerted LB film pressures.

The fractal aggregates behave like wandering rafts on water surfaces,[15] which is compressible by the baffle in an LB trough. At the initial compression step, these aggregates do not contribute substantially to total surface pressures to result in a slow increase in pressure due to the low surface concentration of fractal aggregates as shown in Figure 4.However, a subsequent rapid increase in surface pressure shows strong aggregate−aggregate interactions. The strong aggregate−aggregate interactions result in coalescence of fractal aggregates into larger aggregate-based networks at intermediate surface pressures. Interestingly, the networks are also fractal in structure on the centimeter-to-micrometer scales as shown in Figure 5. Analysis of Figure 5c gives a fractal dimension of ∼1.67 (see the Supporting Information). Insight into the interior of the networks shows that originally generated aggregates are robust, and their fractal structures are nearly kept as shown in Figure 5d. Around the collapse pressure, a plastic-like thin film formed at the water surfaces with one part on the sidewall of the trough. The film is frail, and outside force will result in its partial breaking and subsiding into water. Sometimes, the films will fold to form gold wires. Figure 6 shows a typical photograph of the fished out films. The black wires correspond to the fold films with a color to the naked eye of navy blue, which shows that gold nanoparticles do not fuse into bulk gold with a golden reflectance.

The transfer efficiency of fractal aggregates from the air/water interface onto a solid surface is critically dependent on surface pressures. Figure 7 shows UV−vis absorbance spectra of transferred nanoparticle films on a glass slide at different surface pressures. The maximum surface plasmon resonant bands for these tranferred nanoparticle films are all located at 620 to ∼720 nm, and the increase in surface pressure evidently strengthened the absorbance intensity. Compared with the resonant peak of gold nanoparticles in choroform solution (∼527 nm, dash line in Figure 7), all the resonant peaks in the LB films shift significantly to red. The red-shifted and widening surface plasmon bands demonstrate extensive aggregation of gold nanoparticles.[15] The elevated surface pressures did not result in a further red-shift and widening in the surface plasmon band, indicating that the interior structure of the aggregate (for example, particle-to-particle distance) does not change with increased surface pressure; the enhancing surface pressure increases only the local nanoparticle density. These plasmonic properties correlate with the above discussions on film morphologies. Due to weak interactions between nanoparticle surfaces and CTAB ligands, dampening of surface plasmon

Figure 6. An optical microscope image of the fished out film at the collapse pressure.

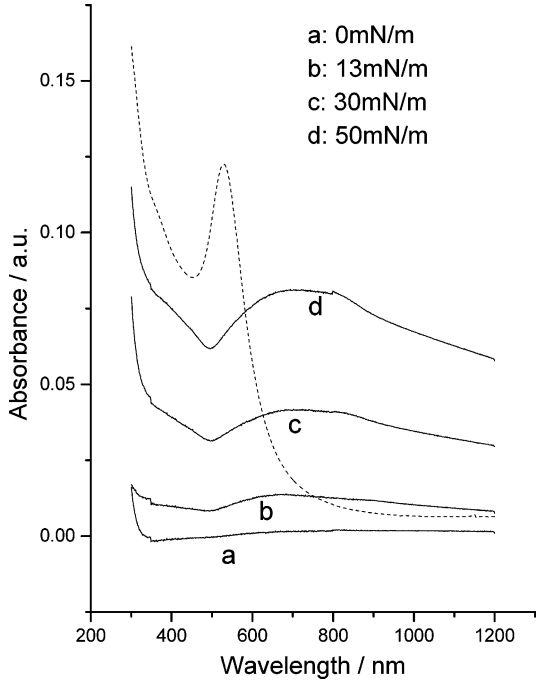

Figure 7. UV−vis absorbance spectra of transferred nanoparticle films on glass at different surface pressures. The dashed line corresponds to the spectrum of unaggregated nanoparticles in chloroform, whose intensity is reduced by 12 times for clear comparison.

absorbance intensity was weaker than that for alkylthiol[11] and alkylamine[18] ligands. Therefore, a fractal-like arrangement of strong surface plasmon polaritons (SPPs) would be expected, which confines the optical energy around nanoparticle chains.[20] It was expected that the method reported here might result in applications, such as nanoscale optical devices relying on SPPs or surface-enhanced Raman scattering from strong local electromagnetic fields.

Conclusion

As-synthesized CTAB-capped gold nanoparticles were found to aggregate spontaneously and rapidly into fractal structures upon spreading them on a water surface. This is different from the case for alkylthiol- or alkylamine-capped metal nanoparticles, which might be due to weak interactions between CTAB and gold surfaces. The fractal aggregates can walk randomly on water surfaces, and they are highly compressible. As a result, gold fractal structures on the centimeter-to-micrometer scales were fabricated successfully aided by LB baffles. In addition, the fractal aggregates were robust, and their structures were kept at intermediate surface pressures.

Acknowledgment. This work was supported by the National Science Foundation of China. (Nos. 20275037, 29975028). We also thank Professor Haishui Wang and Mrs. Yibing Wang for kind help in using their KSV 5000 Langmuir machine.

Supporting Information Available: Figures of analysis results for morphologies shown in Figure 1 and Figure 5c. This material is available free of charge via the Internet at http://pubs.acs.org.

References and Notes

(1) Mandelbrot, B. *The Fractal Geometry of Nature*; Freeman: San Francisco, CA, 1982.

(2) Special Issue for Diffusion-Limited Aggregation and Dendritic Growth. *Phys. Rev. A* **1992**, *45*, 1018−1072.

(3) For example: (a) Wang, Z. H.; Moskovits, M.; Shalaev, V. M.; Suh, J. S.; Botet, R. *Phys. Rev. Lett.* **1994**, *72*, 4149 and references therein. (b) Wenseleers, W.; Stellacci, F.; Meyer-Friedrichsen, T.; Mangel, T.; Bauer, C. A.; Pond, S. J. K.; Marder, S. R.; Perry, J. W. *J. Phys. Chem. B* **2002**, *106*, 6853. (c) Tsai, D. P.; Kovacs, J.; Safonov, V. P.; Shalaev, V. M.; Markel, V. A.; Danilova, Y. E.; Lepeshkin, N. N.; Kim, W.; Rautian, S. G.; Armstrong, R. L. *Phys. Rev. Lett.* **1998**, *80*, 1102.

(4) (a) Stockman, M. I.; Shalaev, V. M.; Moskovits, M.; Botet, R.; George, T. F. *Phys. Rev. B* **1992**, *46*, 2821. (b) Moskovits, M.; Suh, J. S. *J. Phys. Chem.* **1984**, *88*, 5526. (c) Feilchenfeld, H.; Siiman, O. *J. Phys. Chem.* **1986**, *90*, 4590. (d) Siiman, O.; Feilchenfeld, H. *J. Phys. Chem.* **1988**, *92*, 453. (e) Zhang, H. G.; Liu, F. Z.; He, T. J.; Xin, H. W. *Sci. China, Ser. B: Chem.* **1994**, *37*, 395. (f) Yamaguchi, Y.; Weldon, M. K.; Morris, M. D. *Appl. Spectrosc.* **1999**, *53*, 127.

(5) Moskovits, M.; Suh, J. S. *J. Phys. Chem.* **1984**, *88*, 5526.

(6) (a) Weitz, D. A.; Oliveria, M. *Phys. Rev. Lett.* **1984**, *52*, 1433. (b) Félidj, N.; Lévi, G.; Pantigny, J.; Aubard, J. *New. J. Chem.* **1998**, *22*, 725.

(7) Safonov, V. P.; Shalaev, V. M.; Markel, V. A.; Danilova, Y. E.; Lepeshkin, N. N.; Kim, W.; Rautian, S. G.; Armstrong, R. L. *Phys. Rev. Lett.* **1998**, *80*, 1102.

(8) Souza, G. R.; Miller, J. H. *J. Am. Chem. Soc.* **2001**, *123*, 6734.

(9) (a) Schmid, G.; Lehnert, A. *Angew. Chem., Int. Ed. Engl.* **1989**, *28*, 180. (b) Taylor, M. D. R.; Poriarty, P.; Brust, M. *Chem. Phys. Lett.* **2001**, *348*, 27. (c) Mandal, S.; Phadtare, P. R.; Selvakannan, R.; Sastry, M. *Nanotechnology* **2003**, *14*, 878.

(10) Jin, Y.; Dong, S. J. *Angew. Chem., Int. Ed.* **2002**, *41*, 1040; **2002**, *114*, 1082.

(11) (a) Heath, J. R.; Knobler, C. M.; Leff, D. V. *J. Phys. Chem. B* **1997**, *101*, 189. (b) Hassenkam, T.; Nørgaard, K.; Iversen, L.; Kiely, C. J.; Brust, M.; Bjørnholm, T. *Adv. Mater.* **2002**, *14*, 1126.

(12) Yang, P. *Nature* **2003**, *425*, 243.

(13) (a) Meguro, K.; Torizuka, M.; Esumi, K. *Bull. Chem. Soc. Jpn.* **1988**, *61*, 341. (b) Meguro, K.; Tano, T.; Torigoe, K.; Nakamura, H.; Esumi, K. *Colloids Surf.* **1989**, *34*, 381. (c) Wilcoxon, J. P.; Williamson, R. L.; Baughman, R. *J. Chem. Phys.* **1993**, *98*, 9933. (d) Brust, M.; Walker, M.; Bethell, D.; Schiffrin, D. J.; Whyman, R. *J. Chem. Soc., Chem. Commun.* **1994**, 801.

(14) Cheng, W. L.; Dong, S.; Wang, E. *Langmuir* **2003**, *19*, 9434.

(15) The extensive aggregation of gold nanoparticles would result in color changes from red to blue, which have been reported by many groups including us.

(16) (a) Rabani, E.; Reichman, D. R.; Geissler, P. L.; Brus, L. E. *Nature* **2003**, 426, 271. (b) Rabani, E.; Egorov, S. A. *Nano. Lett.* **2002**, 2, 69. (c) Rabani, E.; Egorov, S. A. *J. Chem. Phys.* **2001**, *115*, 3437.

(17) Liu, J.; Shih, Y.; Sarikaya, M.; Aksay, I. A. *Phy. Rev. A* **1990**, *41*, 3206.

(18) (a) Zhou, X. H.; Liu, C. Y.; Jiang, L.; Li, J. R. *Colloids Interfaces, A* **2004**, *248*, 43. (b) Lu, Y.; Liu, G. L.; Lee, L. P. *Nano. Lett.* **2005**, *5*, 5.

(19) (a) Korgel, B. A.; Fitzmaurice, D. *Adv. Mater.* **1998**, *10*, 661. (b) Tang, Z. Y.; Kotov, N. A.; Giersig, M. *Science* **2002**, *297*, 237.

(20) Maier, S. A.; Kik, P. G.; Atwater, H. A.; Meltzer, S.; Harel, E.; Koel, B.; Requicha, A. G. *Nat. Mater.* **2003**, *2*, 229.